Sustainable Extraction and Processing of Raw Materials, 2026

EFFICIENCY AND SELECTIVITY OF COPPER PRECIPITATION AS COPPER OXALATE FROM SOLUTIONS FROM THE MINING INDUSTRY

Plamen Georgiev, Marina Nicolova

University of Mining and Geology "St. Ivan Rilski", 1700 Sofia; E-mail: ps_georgiev@mgu.bg
Corresponding author: ps_georgiev@mgu.bg

ABSTRACT. The aim of this study was to investigate the effect of calcium and ferrous iron ions on the removal of copper-to-copper oxalate from a model solution containing 0.0069 M Cu^{2+}. Copper oxalate was synthesised under optimal experimental conditions (solution pH of approximately 2.5, temperature of 50 °C, and a stirring rate of 250 rpm). This was an effective process for removing copper from the model solution, and the resulting particles were larger than 200 µm and exhibited excellent filtration characteristics. In contrast, higher concentrations of calcium ions (0.036 M) and ferrous iron ions (0.045 M) decreased the selectivity and efficiency of copper removal, respectively.

Key words: copper, pregnant solutions, copper oxalate, selectivity

Introduction

Hydrometallurgy is widely applied to recover base metals from low-grade raw materials and industrial wastes, whose chemical composition and mineralogy make classical processing methods inefficient. In that case, the base metal leaches from the mineral structure and accumulates in the pregnant leach solution. That process is usually nonselective, and the leaching and accumulation of calcium, iron, aluminium, and silicon in solution accompany it. Therefore, processing the pregnant leach solution, the final step in the relevant hydrometallurgical method, aims to obtain a product with higher base-metal content. The most common approaches for separating and concentrating the base metal from the leach solution and transforming it into a higher-purity market product are solvent extraction, stripping, and electrowinning (Shlesinger et al., 2021). However, chemical reduction using scrap remains a suitable method for recovering copper ions from mining solutions in some cases (Li et al., 2024).

Oxalic acid is a natural product of the metabolism of a wide range of heterotrophic microorganisms (bacteria and fungi), plants and animals. Its role is to enhance acidolysis of minerals within their microenvironment and, in turn, to support and regulate the mineral nutrition of organisms (Palmieri et al., 2019).

Oxalic acid has attracted the attention of hydrometallurgists for many years as an efficient and selective agent for recovering base metals from various types of pregnant solutions (Gyliene et al., 1997; Gylliene & Saulkaskas, 1994). Based on its unique chemical properties, oxalic acid is used as a leaching and recovery agent for a wide range of primary raw materials such as lithium-bearing sediments (Tita et al., 2025), slag (Cheng et al., 2026), coal (Zeng et al., 2026), hydroxysulphate and silicate (Krajanova & Lalinska-Volekova, 2025) or spent products, such as spent ion batteries (Martins et al., 2023; Botta et al., 2025), diodes (Mustafa et al., 2025), spent catalysts (Verma et al., 2019), as well as to recover zinc (Lee et al., 2017), some critical elements such as cobalt (Aref et al., 2026), nickel (Yang et al., 2020), and rare earth elements (Wen et al., 2025).

To study the effect of calcium and ferrous iron ions concentration on the removal of copper-to-copper oxalate from a model solution containing 0.0069 M Cu^{2+} was the main aim of this study.

Materials and methods

Precipitation of copper ions to copper oxalate

The reagent-grade salts of $CuSO_4.5H_2O$, $CaCl_2$, and $FeSO_4.7H_2O$ were used in the experiments to prepare a model solution with a composition similar to that of waste or pregnant solutions from the mining industry or biohydrometallurgy. The concentration of Cu^{2+} in all experiments was 440 mg/ L (0.0069 M), while the concentration of Ca^{2+} and Fe^{2+} varied between 275 mg/ L – 1440 mg/ L (0.0069 M – 0.036 M) and 500 mg/ L – 2500 mg/ L (0.0089 M – 0.045 M), respectively. The amounts of the salts needed for the relevant experiment were dissolved in distilled water acidified with sulphuric acid. pH of the prepared solutions ranged from 2.38 to 2.59.

The amount of oxalate ions, $[C_2O_4^{2-}]$, needed to precipitate Cu^{2+} as oxalate was calculated according to the relevant equation:

$$[C_2O_4^{2-}] = (K_{spCuC2O4.H2O})/[Cu^{2+}] \quad (1)$$

where K_{sp} is the solubility product of copper oxalate (Table 1), while $[Cu^{2+}]$ is the copper concentration in solution, M.

Table 1. *K_{sp} values of some oxalates (Rumble, 2018)*

Compound	K_{sp} value at 25 °C
$CuC_2O_4.H_2O$	$4.43.10^{-10}$
CaC_2O_4	$2.3.10^{-9}$
$FeC_2O_4.2H_2O$	$2.1.10^{-7}$

The selective precipitation of cupric ions to copper oxalate was carried out on a magnetic stirrer at 250 rpm and at a constant temperature of 50 °C. After reaching the temperature, the initial pH was measured. The required amount of oxalic acid for the precipitation of cupric ions was divided into five portions and added to the solution at 10-minute intervals. The entire experiment lasted 60 minutes. The pH of the suspension was

measured at 50 °C and at 9.8 °C after the suspension was cooled in an ice bath.

The particles formed at the end of the experiment were separated by vacuum filtration through Blue Ribbon filter paper with a pore size of 2-3 µm. The filtrate was passed through a 0.45 µm membrane filter. The residual concentrations of Cu^{2+}, Ca^{2+}, and Fe^{2+} in the second filtrate were determined by AAS (Perkin Elmer 5000).

Characterisation of the precipitates obtained from the experiments

The efficiency of copper ions removal to copper oxalate ($E_{Cu,\ \%}$) was calculated according to the following formula:

$$Ecu = \frac{C1-C2}{C1} \times 100, \% \quad (2)$$

where C_2-copper ions concentration in the filtrate obtained after membrane filtration, mg/ L; C_1-copper ions concentration in the model solution, mg/ L.

The precipitate deposited on the filter paper was washed with distilled water, dried at 105 °C for 2 hours, and weighed on a precise balance.

The mineralogical composition of the obtained precipitates was determined using a Phillips PW 1050 X-ray Diffraction analyser with Cu anode, operated at 112 kV and 31 mA. The chemical analysis of the obtained precipitates and their surface morphology were carried out using an electron microscope, JEOL JSM-6010 PLUS/LA.

Selectivity of copper precipitation as copper oxalate (S, %) was calculated according to the following formula:

$$\boldsymbol{S} = \frac{Ccu2}{Ccu1} \times 100 \quad (3)$$

where C_{Cu2} – average copper content in the precipitate, determined by the EDS analysis, in the presence of other cations (calcium or ferrous iron) in the solutions; C_{Cu1} – average copper content in the precipitate, determined by the EDS analysis, in the absence of other cations in the solution.

Results and discussion

The rate of copper precipitation to copper oxalate is a pH-dependent. At a pH around 2.5, oxalic acid exists mainly in the non-protonated form, with about 2.0% of the added oxalic acid present as oxalate anions (Verma et al., 2019). Therefore, to maintain the higher rate of copper precipitation, the process was carried out at 50 °C in one hour:

$$Cu^{2+} + (COO)_2^{-} \rightarrow CuC_2O_4 \quad (4)$$

Removal of the oxalate anions from the solution enhances further dissociation of oxalic acid into the relevant anions:

$$(COOH.COOH) \leftrightarrow (COOH.COO^{-}) + H^{+}$$

$$(COOH.COO^{-}) \leftrightarrow (COO^{-}.COO^{-}) + H^{+} \quad (5)$$

Characteristics of copper oxalate

Oxalate anions react with copper ions in the model solution at a higher rate and with almost 100% efficiency (Table 2), forming a readily separable slurry consisting of a light blue, easily filterable precipitate. The electron microscope revealed the formation of irregularly shaped particles with a flat surface, with a predominance of sizes larger than 200 µm (Figure 1). The XRD pattern showed the presence only of the moolooite, copper oxalate ($CuC_2O_4.H_2O$), a mineral consisting of orthorhombic crystals. It forms distinctive peaks at 23, 38-39, 52, 60, 72-78 °Theta positions (Figure 2).

Table 2. *Efficiency of copper ions precipitation under relevant experimental conditions*

Composition of the model solution	Final pH (at 9.8 °C)	Yield of precipitate, g/ L	Residual $[Cu^{2+}]$ after a membrane filtration, mg/ L	$E_{Cu,\ \%}$
0.0069 M Cu^{2+}	1.56	1.15	< 1.5	99.6
0.0069 M Cu^{2+} + 0.0069 M Ca^{2+}	1.62	1.01	42.2	90.4
0.0069 M Cu^{2+} + 0.023 M Ca^{2+}	1.68	0.85	90.2	79.5
0.0069 M Cu^{2+} + 0.036 M Ca^{2+}	1.64	0.68	129.4	70.6
0.0069 M Cu^{2+} + 0.0069 M Fe^{2+}	1.47	0.35	218	50.4
0.0069 M Cu^{2+} + 0.01 M Fe^{2+}	1.58	0.24	295	32.9
0.0069 M Cu^{2+} + 0.045 M Fe^{2+}	1.64	0.11	350	20.4

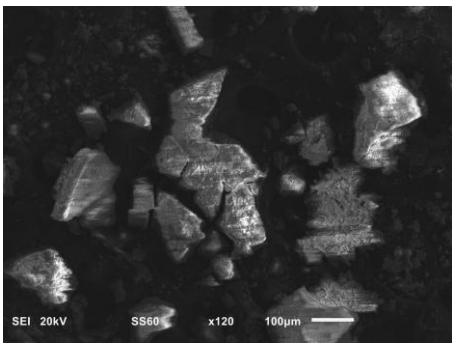


Fig. 1. SEM morphology of copper oxalate obtained from a solution containing 0.0069 M copper

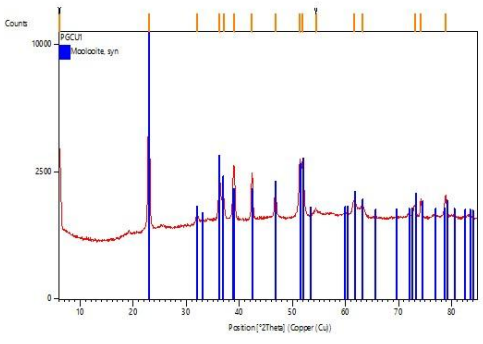
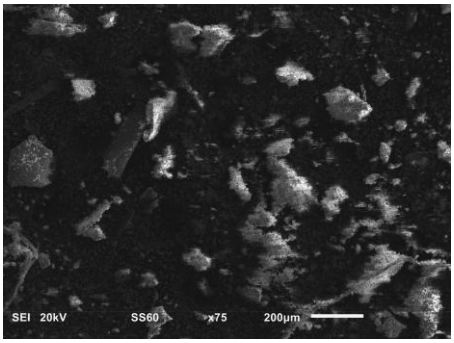
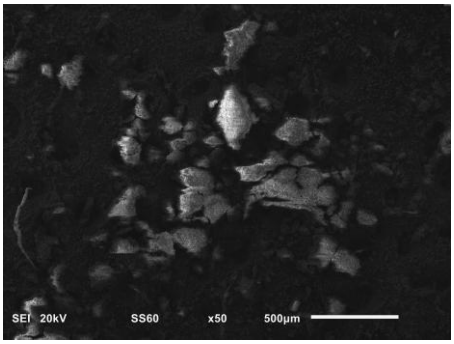


Fig. 2. XRD pattern of precipitates obtained from a solution containing 0.0069 M copper



(a)



(b)

Fig. 3. SEM morphology of precipitates obtained from a solution containing: 0.0069 M copper and 0.023 M calcium (a); 0.0069 M copper and 0.036 M calcium (b)

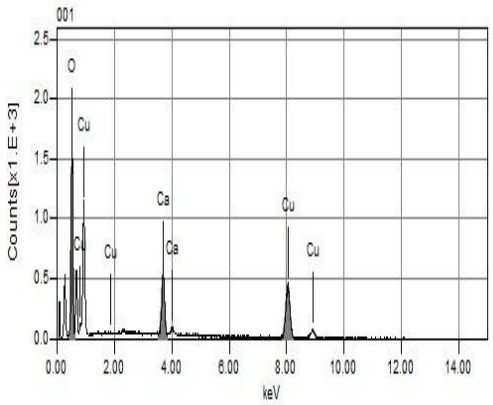


Fig. 4. EDS analysis of the precipitate from a solution containing 0.0069 M copper and 0.036 M calcium

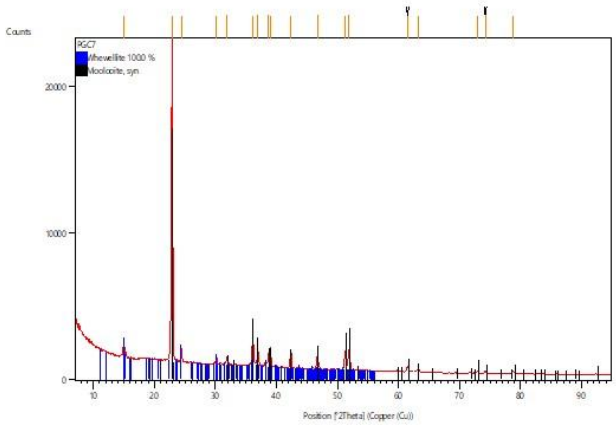


Fig. 5. XRD pattern of precipitates obtained from a solution containing 0.0069 M copper and 0.036 M calcium

The average copper content of copper oxalate, produced from a solution containing only copper, determined by EDS analysis, was 82.3%.

Copper oxalate could be used as a precursor for obtaining high-purity metallic copper, copper oxide, or advanced ceramics such as $CaCu_3Ti_4O_{12}$, which are applied in electronics and energy storage (Chen et al., 2018), or as a protective layer on historical bronze statues (Joseph et al., 20212).

Effect of calcium ions on the copper oxalate formation

Calcium ions in wastewater from the mining industry or biohydrometallurgy result from the chemical neutralisation of sulphuric acid generated or added to the raw material being processed with carbonates. The deposition of gypsum ($CaSO_4 \cdot 2H_2O$) is a key process that prevents the accumulation of high concentrations of calcium ions in waters.

A study (Werner et al., 2021) showed that calcium ions affected primary aggregation and crystallisation pathways of copper oxalate. Therefore, calcium oxalate formation could be minimised by precise control of the addition of oxalate anions. Due to the close K_{sp} values of both oxalates (Table 1), oxalic acid was added to the model solution serially at even intervals of time. It allowed initiating the copper precipitation process without exceeding the oxalate anion concentration required to initiate calcium oxalate formation. However, the experiment carried out at equimolar concentrations of copper and calcium showed a decrease of approximately 10% in the yield of precipitate and in the process efficiency (Table 2).

The precipitation of 0.0069 M Cu^{2+} as copper oxalate in the presence of 0.023 M or 0.036 M Ca^{2+} also resulted in the formation of light-blue particles, which filtered at a higher rate through Blue-Ribbon filter paper. Electron microscopy revealed that the particles still had an irregular shape but now also had a grainy surface. In the presence of 0.023 M Ca^{2+}, the size of deposited particles remained near to 200 µm (Figure 3a). In comparison, in the presence of 0.036 M Ca^{2+}, a significant proportion of the synthesised particles had a size close to 100 µm (Figure 3b). However, the yield of copper oxalate steadily decreased compared to the yield obtained from the experiment in the absence of calcium ions. It reached 59.1% in the presence of 0.036 M Ca^{2+} (Table 2). The fine particles smaller than 2-3 µm formed under these conditions accounted for about 12.7% from the initial copper concentration.

EDS analysis on three distinctive dots on the surface of analysed particles obtained from a model solution containing 0.036 M Ca^{2+}, showed that the average calcium content in precipitates was 9.3% (Figure 4, Table 3). It is evident that, due to their similar ionic radii, calcium ions co-precipitate to some extent with copper ions during the formation and growth of copper oxalate nuclei despite the applied experimental approach.

Notwithstanding a single order-of-magnitude difference in the K_{sp} values of copper and calcium oxalates and the applied experimental conditions, when the calcium concentration in the model solution was five times higher than the copper concentration, the selectivity of copper precipitation was 71.7% (Table 4).

The XRD pattern showed the presence of the moolooite, copper oxalate (CuC_2O_4 H_2O) and whewellite (CaC_2O_4 $2H_2O$) (Figure 5), the most common form of calcium oxalate (Werner et al., 2021). It has a monoclinic crystal structure and exhibits distinctive peaks at 14.9, 24.4, and 30.1 °2θ. However, the peak heights were distinctly lower than those of moolooite.

Table 3. *Chemical composition of the precipitate obtained from the solution containing 0.0069 M copper and 0.036 M calcium ions in three selected points (based on EDS analysis)*

Element	Content, %			Average value	Deviation
	1	2	3		
Cu	45.1	69.0	62.8	59.0	10.1
Ca	8.1	10.3	9.4	9.3	0.9
O	46.8	20.7	27.8	31.7	11.0

Table 4. *Effect of the calcium and ferrous iron ions on the selectivity of copper precipitation as copper oxalate*

Cation	Concentration, M	Selectivity coefficient, %
Ca^{2+}	0.036	71.7
Fe^{2+}	0.045	98.5

Bohner et al. (2014) showed that the selectivity of copper synthesis in the presence of calcium ions depends on the mixing rate, which enhances the complexation and precipitation kinetics of copper ions.

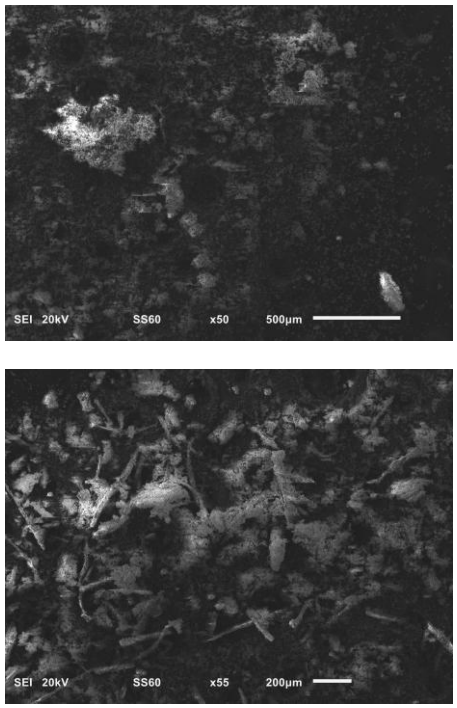
Effect of ferrous iron ions concentration on the copper oxalate formation

Acidic leaching of ferric iron oxyhydroxides and oxidation of sulphides are the main sources of iron ions (Fe^{2+} and Fe^{3+}) in wastewater from the mining industry and in pregnant leach solutions from biohydrometallurgy. Iron, compared to calcium, can build significant concentrations in the above-mentioned streams, requiring a separate stage for iron removal as part of the flowsheet for their processing. Ferrous and ferric iron ions behave differently in the presence of oxalate ions, as ferrous form precipitate to ferrous oxalate (mineral humboldtine, $FeC_2O_4.2H_2O$), while ferric ions form soluble complexes with the organic anions such as $[Fe(C_2O_4)_3]^{3-}$. Therefore, ferric ions must be removed from the mining solutions using suitable methods (precipitation, solvent extraction, reduction, etc.) before precipitating the raw materials as oxalates. In that case, the highly acidic pH of the solution suppressed chemical oxidation of ferrous iron to the ferric state.

The removal of copper as copper oxalate in the presence of ferrous iron ions could be possible due to the three orders of magnitude difference of their K_{sp} values (Table 1). Therefore, the process was carried out under experimental conditions similar to those used for copper removal in the presence of calcium ions.

The precipitation of 0.0069 M Cu^{2+} as copper oxalate in the tested concentrations of ferrous iron ions resulted in the formation of fine, light-blue particles with no yellow-lemon spots (distinctive appearance of $FeC_2O_4.2H_2O$). These particles filtered more slowly than the precipitates obtained from all other experiments. The yield of precipitate and efficiency of copper removal determined at equimolar concentrations of copper and ferrous iron ions dropped to 30.4 % and 50.4%, respectively, with the lowest values observed in the presence of 0.045 M Fe^{2+} (Table 2). It is well known that cation concentrations directly affect the rate of precipitation and the size of crystals at the next stage (Lee et al., 2022). Therefore, the initial higher concentration of ferrous iron ions resulted in rapid nucleation and a higher population of smaller particles on the one hand, and structural disorder due to their inhibitory effect on polymerisation and the long-range growth of already formed crystals on the other hand (Cismasu et al., 2011).

In this case, electron microscopy showed that the particles were not irregular in shape but were elongated and had a distinctly granular surface, especially particles formed in the presence of 0.045 M Fe^{2+}. In the presence of 0.01 M Fe^{2+}, the dominant size of deposited particles was below 100 μ (Figure 6a). In contrast, in the presence of a higher ferrous ion concentration, the particles deposited on the surface of filter paper formed a layer consisting of fine particles non-separable from each other (Figure 6b). However, despite the low efficiency of copper removal and the low value of copper oxalate yield, the collected precipitate contented minimal amount of iron which resulted in very high process selectivity (Table 5, Figure 7).



(a)

(b)

Fig. 6. SEM morphology of the precipitates obtained from a solution containing: 0.0069 M copper and 0.01 M ferrous iron (a); 0.0069 M copper and 0.045 M ferrous iron (b)

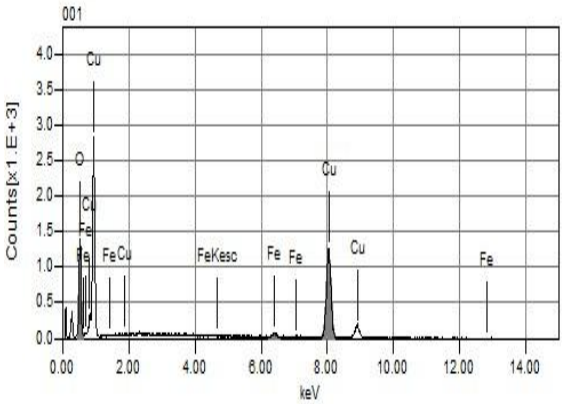


Fig. 7. EDS analysis of the precipitate obtained from a solution containing 0.0069 M copper and 0.045 M ferrous iron

Table 5. *Chemical composition of the precipitate obtained from the solution containing 0.0069 M copper and 0.045 M ferrous iron ions in three selected points (based on EDS analysis)*

Element	Content, %			Average value	Deviation
	1	2	3		
Cu	78.0	83.6	81.9	81.2	2.34
Fe	1.6	1.5	0.6	1.2	0.45
O	20.4	14.9	17.5	17.6	2.25

Mass balance of the copper content in the liquids obtained after sequential filtration through blue ribbon filter paper and a membrane filter with a pore size of 0.45 μm revealed that about 11.4% of the initial base metal content was present in fine particles smaller than 2-3 μm. Several approaches could be applied to increase the yield of larger copper oxalate particles in the presence of ferrous iron ions. Firstly, to increase reaction time and, in this way, enhance the agglomeration of fine particles into larger structures. Secondly, to change the scheme of oxalic acid addition to the solution, combined with maintaining a rate of agitation higher than 240 rpm, to decrease the number of the initially formed nuclei around which growth formed particles with a distinctive structure later.

The XR diffraction pattern revealed the presence of only moolooite, copper oxalate ($CuC_2O_4 \cdot H_2O$), but not humboldtine ($FeC_2O_4 \cdot 2H_2O$) in the precipitate obtained in the experiment (Figure 8). This is likely due to its content below the detection limit of the used diffractometer (2.0 %), or to the formation of crystals with a disordered structure, which makes it difficult to detect using this method (Korneev et al., 2022).

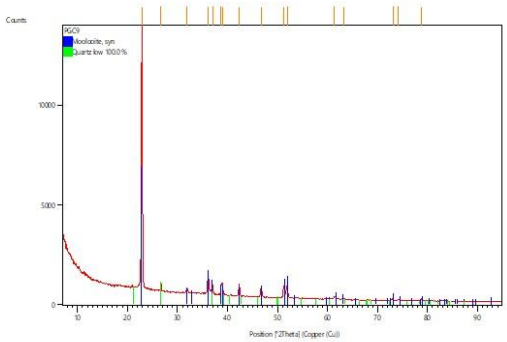


Fig. 8. XRD pattern of precipitates obtained from a solution containing 0.0069 M copper ions and 0.045 M ferrous iron

Conclusion

Calcium content in the model solution, exceeding the equimolar copper content negatively affected the efficiency and selectivity of copper removal as copper oxalate. However, the oxalate obtained from the process consisted of particles larger than 200 μm, which accounted for the high filtration rate. Ferrous iron ion content higher than the equimolar copper content significantly affected copper oxalate synthesis, resulting in particles smaller than 100 μm and reducing the filtration rate. Therefore, the iron content in the mining solution should be removed by suitable methods (oxidation, precipitation, solvent extraction, etc.) before the copper removal to copper oxalate.

Acknowledgements

The authors would like to express their gratitude to the National Science Programme "*Critical and Strategic Raw Materials for a Green Transition and Sustainable Development*", approved by the Resolution of the Council of Ministers № 508/18.07.2024 and funded by the Ministry of Education and Science (MES) of the Republic of Bulgaria, and the Scientific Research and International Partnership Unit of the University of Mining and Geology "St. Ivan Rilski", Sofia (under GPF-260/ 2026 project) for supporting this study.

References

Aref, R., Jantunen, N., & Virolainen, S. (2026). Recovery of high-purity cobalt oxalate from acidic effluents with solvent extraction technology. *Chemical Engineering Science*, *330,* 23878. https://doi.org/10.1016/j.ces.2026.123878

Bohner, B., Schuszter, G., Berkesi, O., Horváth, D., & Tóth, Á. (2014). Self-organization of calcium oxalate by flow-driven precipitation. *Chemical Communications*, *50*(33), 4289–4291. https://doi.org/10.1039/c4cc00205a

Botta, M. P., Attina, B., Ravera, M., & Gabano, E. (2025). Becoming aware of endangered and critical elements: spent batteries as metal mines. *Journal of Chemical Education, 0102 (5), 2103-211.* https://doi.org/10.1021/acs.jchemed.4c01535

Chen, X., Huang, K., & Wang, C. (2018). Facile synthesis of monodispersed copper oxalate flaky particles in the presence of EDTA. *International Journal of Minerals, Metallurgy, and Materials*, *25*(7), 762–769. https://doi.org/10.1007/s12613-018-1624-5

Cheng, S., Vaughan, J., Wang, G., Ma, X., Lyu, X., & Peng, H. (2026). Slag to product: Unlocking titanium-bearing slag value via selective leaching of amorphous titanium phase. *Minerals Engineering, 235*, 109846. https://doi.org/10.1016/j.mineng.2025.109846

Cismasu, A. C., Michel, F. M., Tcaciuc, A. P., Tyliszczak, T., & Brown, J. G. E. (2011). Composition and structural aspects of naturally occurring ferrihydrite. *Comptes Rendus. Géoscience*, *343*(2-3), 210–218. https://doi.org/10.1016/j.crte.2010.11.001

Gylliene, O., & Saulkaskas, M. (1995). Metal recovery from spent electroless plating solutions by oxalate precipitation. *Plating & Surface Finishing*, 61-63.

Gyliene, O., Saulkaskas, M., & Juskenas, R. (1997). The use of organic acids as precipitants for metal recovery from galvanic solutions. *Journal of Chemical Technology & Biotechnology 70*(1), 111-115. https://doi.org/10.1002/(SICI)1097-4660(199709)70:1<111::AID-JCTB691>3.0.CO;2-9

Joseph, E., Cario, S., Simon, A., Wörle, M., Mazzeo, R., Junier, P., & Job, D. (2012). Protection of metal artefacts with the formation of metal–oxalates complexes by Beauveria bassiana. *Frontiers in Microbiology*, *2*. https://doi.org/10.3389/fmicb.2011.00270

Krajanova, V., & Lalinska-Volekova, B. (2025). Hydrometallurgical leaching experiments on selected minerals and materials by oxalic acid. Proceedings of 25 SGEM International Multidisciplinary Scientific GeoConference 2025, 29 June – 06 July 2025 - Albena, Bulgaria, pp. 319-324. https://doi.org/10.5593/sgem2025/1.1/s03.39

Korneev, A. V., Izatulina, A. R., Kuz'mina, M. A., & Frank-Kamenetskaya, O. V. (2022). Solid Solutions of Lindbergite–Glushinskite Series: Synthesis, Ionic Substitutions, Phase Transformation and Crystal Morphology. *International Journal of Molecular Sciences*, *23*(23), 14734. https://doi.org/10.3390/ijms232314734

Lee, K. R., Kim, J., & Jang, J. G. (2017). Recovery of zinc in spent pickling solution with oxalic acid. *Korean Chemical Engineering Research 55*(6), 785-790. DOI:10.9713/kcer.2017.55.6.785

Lee, S. I., Kim, H. R., Park, J. K., J.K., Oh, W., Kim, J., Kim, C., Lee, J., Kim, K.-C., & Lee, B.-C. (2022). Precipitation of ferrous oxalate from ferrous ammonium sulphate in oxalic acid solution. *Processes*, *10*(11), 2420. https://doi.org/10.3390/pr10112420

Li, X., Ma, B., Wang, C., & Chen, Y. (2024). Sustainable recovery and recycling of scrap copper and alloy resources: a review. *Sustainable Materials & Technologies, 41*, e01026. doi.org:1016/j.susmat.2024/e01026

Martins, L. S., Rovani, S., Botelho, A. B. J., & Espinosa, D. C. R. (2023). Sustainable approach for critical metals recovery through hydrometallurgical processing of spent batteries using organic acids. *Industrial & Engineering Chemistry Research*, *62*(44), 18672-18682. https://doi.org/10.1021/acs.iecr.3c03048

Mustafa, L., Usman, M., Ali, S., Ali, A., & Naveed, A. (2025). Recycling technologies for extracting gallium from light-emitting diodes. *Photonics, 12* (8), 808. https://doi.org/10.3390/photonics12080808

Palmieri, F., Estoppey, A., House, G. L., Lohberger, A., Bindschedler, S., Chain, P.S.G., & Junier, P. (2019). Oxalic acid, a molecule, at the crossroads of bacterial-fungal interactions. *Advanced Applied Microbiology,* 106, 49-77. DOI: 10.1016/bs.aambs.2018.10.001

Roy, J. J., Srinivasan, M., & Cao, B. (2021). Bioleaching as an eco-friendly approach for metal recovery from spent NMC-based lithium-ion batteries at a high pulp density. *ACS Sustainable Chemistry & Engineering*, *9*(8), 3060-3069. https://doi.org/10.1021/acssuschemeng.0c06573

Rumble, J. (2018). *CRC Handbook of Chemistry and Physics* (99 ed.). CRC Press. pp. 5–188. ISBN 978-1138561632

Shlesinger, M.E., Sole, K.C., Davenport, W.G., & Alvear Flores, G.R.F. (2021). Extractive metallurgy of copper. (6th ed.). Elsevier. ISBN-13: 978-0128219034

Tita, A.M., Mends, E.A., Kar, U., Hussaini, S., & Chu, P. (2025). Leaching of Li-bearing sedimentary claystones using organic acids. *Green and Smart Mining Engineering*, *2(*2), 156-167. https://doi.org/10.1016/j.gsme.2025.06.002

Verma, A., Kore, R., Corbin, D.R., & Shiflett, M.B. (2019). Metal recovery using oxalate chemistry: a technical review. *Industrial & Engineering Chemistry Research, 58*(34), 15381-15393 https://pubs.acs.org/doi/10.1021/acs.iecr.9b02598#

Wen, Y., Tribby, E.L., & Tang, Y. (2025). Intensified and selective recovery of critical metals from aqueous extracts: Fundamentals and system design. *Chemical Engineering Journal*, *512*, 162661. https://doi.org/10.1016/j.cej.2025.162661

Werner, H., Bapat, S., Schobesberger, M., Segets, D., & Schwaminger, S. P. (2021). Calcium oxalate crystallisation: Influence of pH, energy input, and supersaturation ratio on the synthesis of artificial kidney stones. *ACS Omega*, *6*(39), 26566–26574. https://doi.org/10.1021/acsomega.1c03938

Yang, Y., Song, W., Ferrier, J., Liu, F., Csetenyl, L., & Gadd, G.M. (2020). Biorecovery of cobalt and nickel using biomass-free supernatants from *Aspergillus niger*. *Applied Microbiology & Biotechnology*, *104*, 417-425. DOI: 10.1007/s00253-019-10241-2

Ye, C., Wang, Z., & Shen, Y. (2022). Preparation of iron-copper oxalates and oxides for the oxygen evolution reaction. *Journal of the Electrochemical Society*, *169*, 064503. DOI: 10.1149/1945-7111/ac7259

Zeng, L., Deng, S., Yang, X., & Zhang, W. (2026). Valorisation of pyrite in coal refuse into battery-grade ferrous oxalate: A sustainable pathway. *Chemical Engineering Journal, 534,* 174699. https://doi.org/10.1016/j.cej.2026.174699